

# Gold Nanoparticle Assembly Microfluidic Reactor for Efficient On-line Proteolysis\*<sup>§</sup>

Yun Liu<sup>‡</sup>§, Yan Xue<sup>‡</sup>§, Ji Ji<sup>‡</sup>, Xian Chen<sup>‡</sup>¶, Jilie Kong<sup>‡</sup>, Pengyuan Yang<sup>‡</sup>, Hubert H. Girault<sup>||</sup>, and Baohong Liu<sup>‡</sup>\*\*

A microchip reactor coated with a gold nanoparticle network entrapping trypsin was designed for the efficient on-line proteolysis of low level proteins and complex extracts originating from mouse macrophages. The nanostructured surface coating was assembled via a layer-by-layer electrostatic binding of poly(diallyldimethylammonium chloride) and gold nanoparticles. The assembly process was monitored by UV-visible spectroscopy, atomic force microscopy, and quartz crystal microbalance. The controlled adsorption of trypsin was theoretically studied on the basis of the Langmuir isotherm model, and the fitted  $\Gamma_{\max}$  and  $K$  values were estimated to be  $1.2 \times 10^{-7}$  mol/m<sup>2</sup> and  $4.1 \times 10^5$  m<sup>-1</sup>, respectively. An enzymatic kinetics assay confirmed that trypsin, which was entrapped in the biocompatible gold nanoparticle network with a high loading capacity, preserved its bioactivity. The maximum proteolytic rate of the adsorbed trypsin was 400 nm/(min·μg). Trace amounts of proteins down to femtomole per analysis were digested using the microchip reactor, and the resulting tryptic products were identified by MALDI-TOF MS/MS. The protein mixtures extracted from the mouse macrophages were efficiently identified by on-line digestion and LC-ESI-MS/MS analysis. *Molecular & Cellular Proteomics* 6:1428–1436, 2007.

With the advent of the postgenome era, much attention has been directed toward deciphering the proteome that may correlate to various disease states (1). One of the essential tasks of proteomics is the identification of target proteins in cells or tissues from which information such as protein molecular weight, isoelectric point, sequence, and ultimately the structure facilitates understanding the biological function of a protein (2). The rapid development of mass spectrometry and the associated coupled technologies has provided an opportunity to perform protein and peptide separation and identification in a highly automated and rapid fashion; hence more comprehensive protein mapping in cells or tissues can be

obtained. Prior to protein characterization by mass spectrometry analysis, it is necessary to perform the controlled enzymatic degradation of protein samples to form specific fragments. The conventional digestion process suffers from limitations of long digestion time, chronic autodigestion of enzyme, and sample loss, which affect the proteolytic efficiency and prevent further subsequent positive identification of the proteins of interest. To overcome these disadvantages, many techniques have been recently developed. Toyo'oka and co-workers (3) prepared a trypsin-encapsulated enzyme reactor by the sol-gel method integrated into capillary electrophoresis showing good enzymatic activity for low molecular weight substrates. Slys *et al.* (4) reported a facile technique using a column system that conducted a sensitive tryptic digestion, which required subnanogram quantities of standard proteins. Nevertheless the digestion of unknown proteins in very small volumes, associated with tissues, cells, subcellular compartments, and exocytosis, still remains a challenge (5).

Microfluidic chips have been widely recognized as a powerful technology that will play an important role in future biological analysis to meet the large scale and high throughput requirements (6). Their miniaturized architectures provide a number of distinct advantages, such as high sample processing rates, low manufacturing costs, advanced system integration, and reduced volumes of samples and analytes (7). In particular, microfluidics technology enables the implementation of miniaturized platforms containing immobilized enzymes, contributing to the enhancement of proteolytic efficiency in a shortened incubation time for on-line proteome analysis (8). In contrast to bead-filled capillaries, the number of theoretical plates is higher for open microchannel devices because the flow is more uniform. Besides the pressure drop across an open microchannel system is much less than that for a packed column. Slys *et al.* (4) proposed that a chip-based design would be used in their subsequent study. Commercial polymer materials, such as poly(methyl methacrylate), poly(dimethylsiloxane), and poly(ethylene terephthalate), have been widely used in the large scale manufacture of microdevices due to the low cost and diverse chemical and mechanical properties. However, the poor biocompatibility properties of polymers are not advantageous for the immobilization of enzymes and biomolecules. Therefore, surface modification is a critical issue in the design of polymeric microdevices for

From the <sup>‡</sup>Department of Chemistry and Institute of Biomedical Sciences, Fudan University, Shanghai 200433, China, <sup>¶</sup>Department of Biochemistry and Biophysics School of Medicine, University of North Carolina, Chapel Hill, North Carolina 27599, and <sup>||</sup>Laboratoire d'Electrochimie Physique et Analytique, Ecole Polytechnique Fédérale de Lausanne, CH-1015 Lausanne, Switzerland

Received, October 16, 2006, and in revised form, May 16, 2007  
Published, MCP Papers in Press, May 22, 2007, DOI 10.1074/mcp.T600055-MCP200

bioanalysis. Many efforts have been devoted to chemically functionalizing and patterning biocompatible surfaces to immobilize biologically active compounds. POROS beads have a very good affinity for protein or peptides. Pearson and co-workers (9) developed a new flow cytometry method allowing the rapid assessment of large numbers of particle-bound antibodies. Protein G-derivatized POROS beads were used to bind affinity-purified antibodies specific for synthetic peptides designed from human plasma proteins. Fréchet and co-workers (10, 11) prepared the enzymatic microreactors in capillaries by immobilizing trypsin on porous polymer monoliths. In our group, several methods including sol-gel entrapment, layer-by-layer assembly, covalent binding, and physical adsorption have been proposed to modify the surfaces of microfluidic channels that are further utilized to entrap enzyme and target proteins for protein identification and chiral analysis (12–15).

Because of its good biocompatibility, charge-stabilized gold nanoparticles (AuNPs)<sup>1</sup> provide a mild microenvironment similar to that of proteins in native states and give the protein molecules more freedom in orientation. They are biocompatible and nontoxic and can offer large specific surface areas for ready binding of a large range of biomolecules such as amino acids, proteins, and antibodies (16). In this study, poly(diallyldimethylammonium chloride) (PDPA)/AuNP multilayer films containing protease were assembled on the surface of poly(ethylene terephthalate) (PET) microchannels to obtain a flow-through protein digestion biochip. Sequential alternate adsorption of the cationic polyelectrolyte PDPA and the anion-coated AuNPs led to the formation of a biocompatible and large specific surface-to-volume ratio network to immobilize the enzymes. Coupled with MALDI-TOF MS or two-dimensional LC-ESI-MS/MS, low level protein samples (16 fmol) and complex proteins extracted from the mouse macrophages were identified. This strategy offers a simple and easy-to-use protocol toward implementing fast, efficient, and on-line digestion that is required for the further development of proteomics.

## EXPERIMENTAL PROCEDURES

### *Materials and Chemicals*

PET sheets (100  $\mu\text{m}$  thick, Melinex) were purchased from DuPont (Geneva, Switzerland). PDPA was obtained from Sigma. BSA, cytochrome c, myoglobin, ovalbumin, and trypsin (EC 3.4.21.4 from bovine pancreas) were obtained from Sigma. All other chemicals were of analytical grade and purchased from the Shanghai Chemical Reagent Co. (Shanghai, China).

<sup>1</sup> The abbreviations used are: AuNP, gold nanoparticle; PDPA, poly(diallyldimethylammonium chloride); PET, poly(ethylene terephthalate); QCM, quartz crystal microbalance; BAEE,  $\alpha$ -N-benzoyl-L-arginine ethyl ester; Cyt-c, cytochrome c; SCX, strong cation exchange; RP, reverse-phase; OVA, ovalbumin; PMF, peptide mass fingerprint; IPI, International Protein Index.

### *Cell Culture and Protein Extraction*

The macrophage cell line AMJ2-C8 (from ATCC, CRL-2455) was cultured in high glucose Dulbecco's modified Eagle's medium supplemented with 10% fetal bovine serum, 100 units/ml penicillin, and 100  $\mu\text{g}/\text{ml}$  streptomycin and incubated at 37 °C in a 5%  $\text{CO}_2$  atmosphere. The grown cells were harvested, washed with ice-cold PBS twice, and stored at -80 °C. The proteins were extracted by two different solvents with protease inhibitor mixture: one was water, and the other was 4 M urea. The obtained proteins were digested, separated, and analyzed, respectively.

### *Fabrication of PET Microfluidic Chips*

The microchip was fabricated by photoablation and thermal lamination as reported previously (17). Briefly the PET sheet was placed on computer-controlled XY translation stages (Physik Instrumente, Karlsruhe/Palmbach, Germany) and scanned to be photoablated by a UV excimer laser (argon-fluorine, 193 nm; LPX 2051, Lambda Physik, Gottingen, Germany) for generating a 2-cm-long channel with a trapezoidal cross-section shape about 42  $\mu\text{m}$  deep and 107  $\mu\text{m}$  wide. The straight line channel has photoablated reservoirs at each end. The microstructured PET was thermally sealed by a polyethylene/PET layer at 110 °C using a lamination machine (Hangzhou Fengling Electronic Instrument Co. Ltd., Zhejiang, China) after the surface modification.

### *Synthesis of AuNPs*

The AuNPs were synthesized according to previous literature (18). In brief, in a 1-liter round bottom flask equipped with a condenser, 500 ml of 1 mM  $\text{HAuCl}_4$  was brought to a rolling boil with vigorous stirring. Rapid addition of 50 ml of 38.8 mM sodium citrate to the vortex of the solution resulted in a color change from pale yellow to burgundy. Boiling was continued for 10 min; the heating mantle was then removed, and stirring was continued for an additional 15 min. The resulting solution of colloidal particles was characterized by an absorption maximum at 520 nm.

### *PET Microchannel Surface Modification and Enzyme Immobilization*

The PET microfluidic chip was rinsed with distilled water and ethanol and then dried at room temperature. PET was hydrolyzed using 1 M aqueous NaOH for 16 min at 60 °C and subsequently protonated to prepare PET-COOH (19). This surface contained both carboxyl and hydroxyl functional groups and was negatively charged at sufficiently high pH 13. After hydrolysis, the PET film was washed with 0.1 M HCl (once), distilled water (twice), and ethanol (once) and dried at reduced pressure. Subsequently the PET film was incubated in PDPA solution (3 mg/ml, containing 0.13 M sodium chloride and 5 mM ammonia) for 20 min to adsorb a layer of positively charged PDPA followed by rinsing with distilled water three times. In the next step, the charge polarity on the surface of the film was reversed by the adsorption of a layer of AuNPs with an incubation time of 40 min followed by rinsing with water. After different numbers of bilayers of PDPA/gold nanoparticle assembly had been deposited, the film was dried at room temperature under reduced pressure. Then the layer-by-layer modified PET chip was soaked in 5 mg/ml trypsin solution containing 50 mM Tris-HCl buffer (pH 8.0) and 20 mM  $\text{CaCl}_2$  for at least 2 h at 4 °C. Subsequently the channel of the PET microchip was sufficiently washed by water.

### Characterization of PDDA/AuNP Multilayer-assembled PET Surface

**UV-Visible Spectroscopy**—The UV-visible adsorption monitoring of the deposition of the subsequent layers of AuNPs was performed on a Shimadzu-2450 UV-visible spectrophotometer.

**Atomic Force Microscopy Imaging**—The surface topography was assessed by atomic force microscopy (electrochemical scanning probe microscope, PicoScan 2100) in tapping mode. Micrometer scanning was performed with nanosensors etched silicon probes. The instrument parameters were set as follows: scan size, 3.5  $\mu\text{m}$ ; resonance frequency, 60–80 kHz. The images were flattened using the Nanoscope software.

**Quartz Crystal Microbalance (QCM) Measurement**—The controlled adsorption amount of trypsin in the coating network was determined *in situ* with a QCM analyzer (CHI420, CH Instruments, Inc.) and quartz crystals (7.995 MHz) sandwiched between two gold electrodes (area, 0.196  $\text{cm}^2$ ). AuNPs, PDDA, and trypsin solution were assembled on the gold surfaces. The adsorption time of PDDA and AuNPs for each deposition step was 20 and 40 min, respectively. After deposition, the gold electrode surface was thoroughly rinsed with pure water and dried under nitrogen gas. The QCM frequency change in air was measured.

### Activity Assay of the Immobilized Trypsin

The activity of the encapsulated enzyme in microchip was examined by flowing  $\alpha$ -N-benzoyl-L-arginine ethyl ester (BAEE) solution (5–20 mM) in a 50 mM Tris-HCl buffer (pH 8.0) through the surface-modified channel using a 74900 Series syringe pump (Cole-Parmer Instrument Co.) at a flow rate of 100  $\mu\text{l}/\text{h}$ . The resulting products were analyzed by a capillary electrophoresis system (P/ACE System 5000, Beckman). The capillary electrophoresis was run in phosphate buffer solution (pH 2.5) at 15  $^\circ\text{C}$  with UV detection at 214 nm. The trypsin activity was calculated via the flow rate and absorbance difference.

### On-chip Standard Protein Digestion and Identification

Standard protein solutions of cytochrome c (Cyt-c), myoglobin, BSA, and ovalbumin (OVA) were dissolved in 10 mM  $\text{NH}_4\text{HCO}_3$  buffer solutions (pH 8.0) and thermally denatured before digestion. The sample solutions were respectively driven through the PDDA/AuNP-assembled microreactor by a 74900 Series syringe pump (Cole-Parmer Instrument Co.) at a flow rate of 120  $\mu\text{l}/\text{h}$ . Peptides that accumulated in the outer reservoir were collected by a digital pipette (2–20  $\mu\text{l}$ , Eppendorf Research) and then analyzed by MALDI-TOF MS. MS experiments were performed on a 4700 Proteomics Analyzer with TOF/TOF optics (Applied Biosystems, Framingham, MA). Each volume of 0.5- $\mu\text{l}$  peptide solutions was dropped on the MALDI plate. After the solvent was evaporated, a volume of 0.5  $\mu\text{l}$  of matrix solution (4 mg/ml  $\alpha$ -cyano-4-hydroxycinnamic acid dissolved in 50% aqueous ACN, 0.1% TFA) was dropped onto the sample layer. The MS instrument was operated at an accelerating voltage of 20 kV. A 200-Hz pulsed neodymium-doped yttrium aluminium garnet (Nd:YAG) laser at 355 nm was used. Before the samples were identified, the MS instrument was calibrated with an external calibration mode by tryptic peptides of myoglobin. All spectra were taken from signal averaging of 800 laser shots with the laser intensity kept constant. GPS Explorer software from Applied Biosystems with MASCOT as a search engine and Swiss-Prot as a database was used to identify proteins. All proteins were identified using the peptide fingerprint mass spectra combined with tandem mass spectra. The peptide mass tolerance was set to 80 ppm, and the tandem mass tolerance was set to 0.5 Da.

### Strong Cation Exchange (SCX)-RPLC-ESI-MS/MS Analysis

Protein identification was performed by LC-nanospray MS/MS analysis using a QSTAR XL mass spectrometer (Applied Biosystems) as described previously by Gu *et al.* (20). Separations of the digested peptides were achieved using an HPLC system (LC Packings, San Francisco, CA) consisting of an autosampler (Famos), a precolumn switching device (Switchos), and an HPLC pump system (Ultimate). Samples (10  $\mu\text{l}$ ) were loaded onto an SCX column (BioX-SCX-90  $\text{\AA}$ , 15  $\text{cm} \times 1000 \mu\text{m}$ ). Peptides were then eluted from the SCX column with a series of ammonium acetate gradients: 0, 50, 100, 200, 400, 800, 1000, and 2000 mM, respectively. Each eluted fraction was on-line separated on a  $\text{C}_{18}$  column (Grace Vydac, 25  $\text{cm} \times 150 \mu\text{m}$ , 300  $\text{\AA}$ ) at a flow rate of 1.2  $\mu\text{l}/\text{min}$ . Buffer A was 5% ACN and 0.1% formic acid; buffer B was 95% ACN and 0.1% formic acid. The gradient separations were increased from 0 to 10% B over 18 min, ramped to 50% B at 125 min, increased to 90% B at 130 min, held at 90% B for 5 min, decreased to 30% B at 140 min, and returned to 0% B at 145 min. As peptides were eluted off the column, they were directly introduced into a QSTAR Pulsar ESI-hybrid quadrupole-TOF instrument (Applied Biosystems/MDS Sciex) and were analyzed using data-dependent switching between MS and MS/MS modes: after a 1-s MS spectrum up to three multiply charged precursor ions could be selected for 3-s MS/MS spectral acquisitions; mass ranges for TOF MS and MS/MS were 400–1600 and 100–2000 Da, respectively. The program AnalystQS (Applied Biosystems) was used for data acquisition and instrument control.

### Database Queries and Protein Identifications

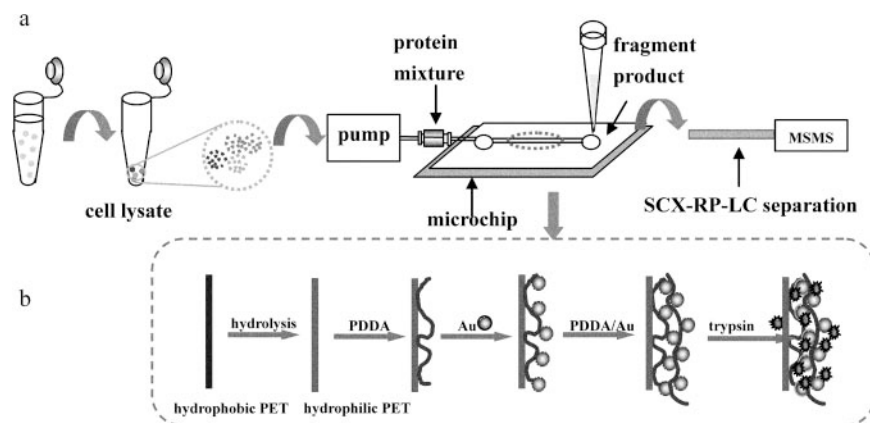
The MASCOT server was used to interpret the LC-MS/MS data by searching against the species of *Mus musculus* from the International Protein Index (IPI) mouse version 3.07 database. The parameters for database searching were set as follows: 1) mass tolerance at  $\pm 0.6$  Da for MS and  $\pm 0.8$  Da for MS/MS, 2) one miscleavage of tryptic enzyme specificity was allowed, 3) charge state from 2 to 3, and 4) no smoothing of spectra was applied. Peptide matches with significant homology ( $p < 0.05$ ) were considered identified peptides. To further increase the degree of confidence of proteins, the reversed IPI mouse version 3.07 database was utilized to evaluate the searching results (21, 22).

## RESULTS AND DISCUSSION

The purpose of this work was to construct a biocompatible stationary phase with large specific surface area to accommodate trypsin on the surface of a microchannel. Because it was reported that entrapped trypsin was more efficient than trypsin in bulk solution (23, 24), the stationary phase was designed to lead to efficient protein digestion and identification. Therefore, the specific features of the PDDA/AuNP multilayer network should provide high affinity for enzyme immobilization but also host the enzymes in a favorable microenvironment. Scheme 1 describes the protocol of enzyme immobilization and further protein identification in the PDDA/AuNP-assembled microchip.

**Characterization of the PDDA/AuNP Assembly and Trypsin Immobilization**—Atomic force microscope images were used to characterize the topographical features of the multilayer assembly on the PET surface (17). The harsh oxidative treatment used to generate surface charges enhances the roughness of the PET surface. Indeed the PET substrate has to be

SCHEME 1. a, workflow schematic diagram of the identification of protein mixture from mouse macrophages by coupling the immobilized enzyme microchip reactor with SCX-RPLC/MS/MS. b, the assembly process of PDDA/AuNP multilayers and trypsin immobilization on the PET microchannel.



chemically treated to generate negatively charged hydrophilic groups ( $\text{OH}^-$  and  $\text{COOH}^-$ ) onto which multilayers of polyelectrolyte PDDA/AuNPs could be alternately adsorbed by electrostatic interactions. After the deposition of the first bilayer of PDDA/AuNPs (Fig. 1a), a few unevenly distributed protrusions could still be observed stemming from the original roughness of the substrate. After the formation of the second bilayer, it can clearly be seen in Fig. 1b that the AuNPs formed a more uniform film smoothing out the original roughness. As the number of bilayers increased, gold nanoparticle aggregation became a predominant factor (Fig. 1c). For the present purpose of forming a scaffold of polyelectrolyte and AuNPs, the observed roughness and inhomogeneity is an advantage for adsorbing enzymes while maintaining easy pathways for substrate access and peptide diffusion. Fig. 1d displays the surface morphology of trypsin-loading bilayers of PDDA/AuNPs showing that the adsorption/desorption of the enzymes did not significantly change the morphology of the network assembly.

To monitor the deposition process of layer-by-layer assembly on the PET substrate, UV-visible spectroscopy was used to measure the absorbance of the gold plasmon band as shown in Supplemental Fig. SI-1. The absorbance intensity increased with the number of AuNP layers. However, a progressive red shift of AuNP maximum absorbance from 536 to 650 nm could be observed upon the successive deposition caused by the aggregation of the particles as the number of layer increases. Such an aggregation will lead to the reduction of the specific surface area, which is not desired for the enzyme immobilization.

**Langmuir Adsorption Isotherm**—Adsorption and transport processes have been mathematically modeled to get a better understanding of the enzyme adsorption process on the multilayer assembly substrates. The model is based on the Langmuir isotherm, which uses the active site concept in the adsorption expression to address the reduction of its rate with the coverage of the wall. The model has found wide applications for the adsorption of proteins on substrates (25, 26). According to the Langmuir isotherm model, the expression relating the concentration of analyte ad-

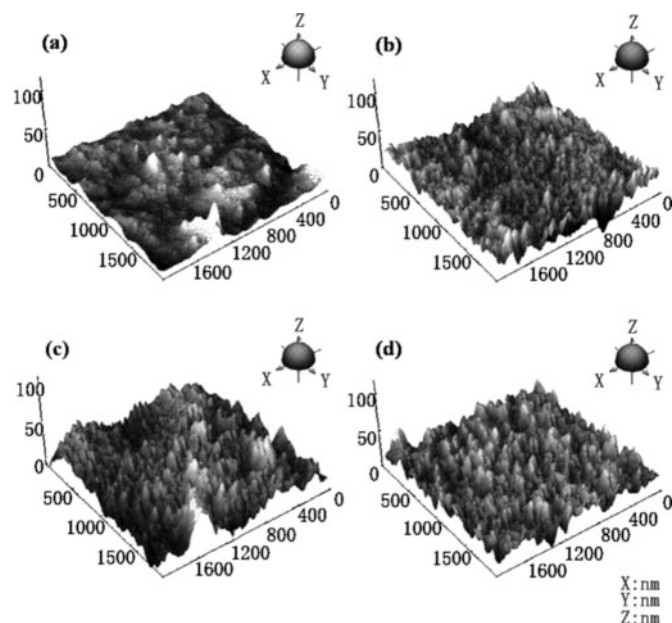


FIG. 1. Atomic force microscopy images (tapping mode) of the modified PET surface. a, one-bilayer PDDA/AuNPs. b, two-bilayer PDDA/AuNPs. c, three-bilayer PDDA/AuNPs. d, trypsin immobilized in the two-bilayer PDDA/AuNPs assembled on the PET surface.

sorbed on the surface  $\Gamma$  to the concentration of analyte in solution C at equilibrium is

$$\frac{\Gamma_{\text{eq}}}{\Gamma_{\text{max}}} = \frac{KC^{\circ}}{1 + KC^{\circ}} \quad (\text{Eq. 1})$$

where  $\Gamma_{\text{eq}}$  is the surface concentration at equilibrium,  $\Gamma_{\text{max}}$  is the initial concentration of the active sites,  $K$  is the thermodynamic constant of adsorption, and  $C^{\circ}$  is the initial concentration of the solution. The adsorption isotherm equation (Equation 1) is linearized as follows.

$$\frac{C^{\circ}}{\Gamma_{\text{eq}}} = \frac{1}{K\Gamma_{\text{max}}} + \frac{C^{\circ}}{\Gamma_{\text{max}}} \quad (\text{Eq. 2})$$

To study the isotherm, we carried out QCM experiments on the electrodes that had been treated as the PET microchannel surfaces. In this way, it was possible to measure the increase

of the mass of the multilayer assembly upon adsorption of proteins from the bulk. The experimental isotherm of trypsin adsorption is shown in Fig. 2 with the linearized isotherm in the *inset line*. Reporting  $C^0/\Gamma_{\max}$  versus  $C^0$ ,  $\Gamma_{\max}$  and  $K$  are provided as the respective reciprocals of the slope and the intercept, giving the fitted values  $\Gamma_{\max} = 1.2 \times 10^{-7}$  mol/m<sup>2</sup> and  $K = 4.1 \times 10^5$  M<sup>-1</sup>. This maximum surface coverage would correspond to an area per molecule of 13 nm<sup>2</sup> in an equivalent compact monolayer. These data clearly show that the assembly provides a bulky sorbent stationary phase for the enzymes. The  $K$  values show that the network scaffold combining a positively charged polyelectrolyte and negatively charged AuNPs can extensively extract proteins from an aqueous solution. These results demonstrate that the assembly coating provides a good structure for the design of a reactor.

**Kinetic Enzyme Activity Assay**—The activities of adsorbed trypsin within different bilayers of PDDA/AuNPs were evaluated by the values of the Michaelis constant ( $K_m$ ) and maximum velocity ( $V_{\max}$ ), both of which are derived from a linear-

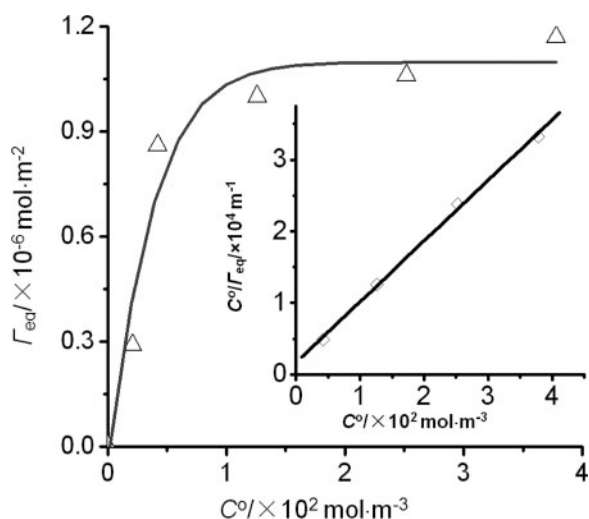
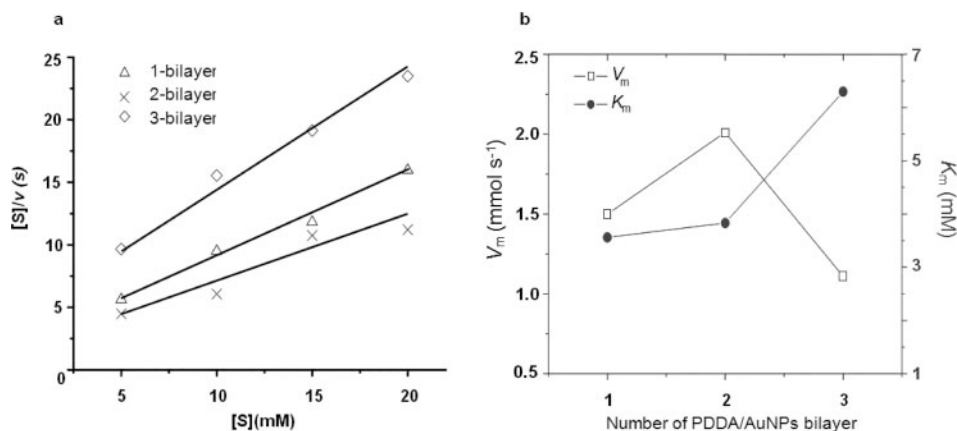


FIG. 2. Isotherm of trypsin adsorption on the PDDA/AuNP multilayer-assembled PET obtained from the QCM experimental results. *Inset line*, linearization of the adsorption isotherm.

FIG. 3. a, Hanes plots for trypsin adsorbed in different bilayers of PDDA/AuNPs on the PET surface. The conditions were: immobilization, 5 mg/ml (w/v) trypsin aqueous solution; determination of activity, 5–20 mM BAEE in 50 mM Tris buffer (pH 7.4). b, variation of the Michaelis constant ( $K_m$ ) and maximum velocity ( $V_{\max}$ ) of immobilized trypsin on different bilayers of PDDA/AuNPs.



ized form of the Michaelis-Menten equation.

$$[S]/v = (K_m)/V_{\max} + (1/V_{\max})[S] \quad (\text{Eq. 3})$$

This equation applies to a bulk solution where  $v$  is the rate of the enzymatic reaction and  $[S]$  is the bulk concentration of substrate in the flowing solution. The  $K_m$  value reflects the enzymatic affinities, and the  $V_{\max}$  value represents the activity of immobilized trypsin in the microreactor. The plots for the conversion of BAEE in the enzymatic microreactors prepared by different bilayers of PDDA/AuNPs are reported in Fig. 3a, and the corresponding kinetic characteristics are shown in Fig. 3b. As can be seen, trypsin immobilized in two PDDA/AuNP bilayers possesses the highest  $V_{\max}$ , which implies that a higher reaction rate for the two-bilayer-coated enzymatic reactor can be achieved than for any other coatings. On the other hand, the  $K_m$  value of the three-bilayer-coated enzymatic reactor is the highest. Enzyme within the two-bilayer assembly showed a maximum reaction rate of 2.0 mM/s, *i.e.* the value of  $V_{\max}$  per unit of trypsin is about 400 mM/(min·μg). Because trypsin is only located on the walls of the bioreactor, this value may reflect the high amount of trypsin present in the microreactor. Additionally the high reaction rate could be attributed to the high surface-to-volume ratio and the microstructured confinement of microchannels. The well defined scaffold assembled by PDDA/AuNPs could provide the high specific surface area for enzyme adsorption and also a biocompatible microenvironment for preserving the bioactivity.

**On-chip Protein Digestion and Identification**—As a consequence of the recent increasing need for new high throughput and automated proteome analysis, our goal in this work was to unite a rapid on-line proteolysis event with the protein identification. Hence using the PDDA/AuNP assembly approach, we developed the enzyme-containing microchip reactor, which enables a high amount of trypsin to be confined within the nanovolume space of a microchannel. Four representative proteins with multiple cleavage sites, BSA (molecular weight = 66,000), OVA (molecular weight = 42,700), Cyt-c (molecular weight = 11,565), and myoglobin (molecular weight = 16,700), were selected to assess the performance of the as-prepared PDDA/AuNP-assembled microreactor.

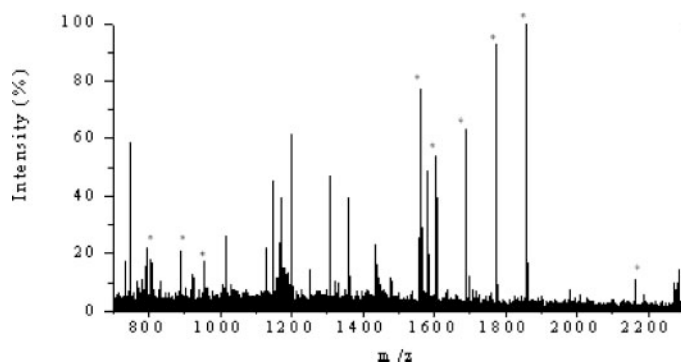


FIG. 4. MALDI-TOF mass spectrum of digests of ovalbumin using PDDA/AuNP multilayer-modified microchip reactor with a flow rate of 4.0  $\mu\text{l}/\text{min}$ . Proteins are 0.20  $\mu\text{g}/\mu\text{l}$  in 10 mM  $\text{NH}_4\text{HCO}_3$  buffer solution (pH 8.1). The eluent-to-matrix ratio is 1:1. The peaks marked with asterisks represent the matched peptides.

As mentioned above, the two-bilayer-assembled enzymatic reactor was capable of conducting the most efficient protein digestion. Next the effect of the number of the assembled bilayers on efficiency of protein digestion was experimentally investigated with 200  $\text{ng}/\mu\text{l}$  BSA using MALDI-TOF-MS. As shown in Supplemental Fig. SI-2, the number of identified peptides varied significantly with the different numbers of bilayers. In the two-bilayer-assembled reactor, 10 peptides digested from BSA were identified, whereas only four peptides could be obtained using the unmodified PET microchannel. Therefore, we further confirmed that the microchip reactor assembled with two bilayers performed with the highest enzymatic efficiency for the following proteolysis of standard and practical proteins of cellular extract samples.

Ovalbumin, a major protein in chicken egg white, is resistant to digestion by trypsin and usually requires thermal denaturation before digestion (27) because this hydrophobic glycoprotein is known to possess a disulfide bridge, one *N*-glycosylation, and four phosphorylation sites (28, 29). In the present study ovalbumin was used as an example for the assessment of the as-prepared on-chip protein analysis. At a flow rate of 4.0  $\mu\text{l}/\text{min}$ , 200  $\text{ng}/\mu\text{l}$  OVA solution was pumped through the miniaturized microchip reactor, which afforded a very short residence time of less than 5 s. The samples collected from the microreactor were deposited onto the MALDI target plate. The MALDI mass spectrum of multilayer-based tryptic digests was free of trypsin autolysis artifacts as displayed in Fig. 4. Detailed identification information is summarized in Supplemental Table SI-1, which shows that nine tryptic peptides were generated from OVA and corresponded to an amino acid sequence coverage as high as 36–41%. The identification results could be comparable to those by in-solution digestion that requires a reaction time of 6 h (30). The results show that trypsin entrapped in the microchannels could act as a good biocatalyst and achieve more rapid reaction.

The as-prepared enzyme microchip reactor was composed

of PDDA/AuNP multilayers forming porous small-sized skeletons and providing a relatively high surface area. Meanwhile the concentration of enzyme relative to protein sample is greatly increased. Normally the proportion of enzyme to protein is about 1:30 because a high enzyme-to-sample ratio often produces a high degree of enzyme autolysis, which can easily mask the signals of the sample peptides in spectrum. To produce adequate cleavages of target proteins at low concentration, some of which are naturally resistant to digestion, conventional tryptic methods require longer a incubation time. The chip-based reactor with immobilized trypsin is a promising option to improve the proteolytic efficiency for low level protein digestion.

2  $\text{ng}/\mu\text{l}$  Cyt-c was used as an example of reduced protein loading for the evaluation of this chip-based reactor. Cyt-c is easy to digest within minutes for in-solution digestion, whereas using the on-chip microreactor, the digestion can be accomplished within a few seconds. Fig. 5a shows the resulting PMF spectrum where 11 tryptic peptides were assigned, corresponding to an amino acid sequence coverage of Cyt-c as high as 68%. It is worth noting that the signal-to-noise ratio of the spectrum was high, and no interfering signals from enzyme autolysis signals could be observed. The identified fragments are listed in Supplemental Table SI-2. With a continuous decrease of the concentration, Cyt-c at 0.5  $\text{ng}/\mu\text{l}$  could also be positively identified with eight peptides and 50% sequence coverage obtained (Fig. 5b). These results reveal that the PDDA/AuNP assembly microchip is especially superior in efficient digestion of trace level proteins (about 16 fmol) per analysis within a very short digestion time. Another example is myoglobin at the concentration of 2  $\text{ng}/\mu\text{l}$ . Using the microchip enzymatic microreactor, six peptides could be identified corresponding to 38% amino acid sequence coverage (Fig. 5c). Currently several techniques have been developed to overcome the limitations of conventional digestion. For example, coupled with the LC-MS system, the enzyme column reactors have been prepared to perform on-line protein identification. However, few of these techniques have been applied to complex samples. To realize rapid and high throughput proteome analysis, the chip-based techniques have been proposed in biological analysis.

*Digestion of the Proteins Extracted from Mouse Macrophages*—The proposed digestion protocol was effectively applied to a real proteome analysis. The proteins extracted from mouse macrophages were identified. Macrophages play an important role in normal development and physiology and the pathogenesis of many diseases (31). In the bone marrow, they are a key component of the stem cell niche and the regulatory stromal microenvironment that controls stem cell biology and blood cell production. An understanding of macrophage biology is therefore important for understanding normal and abnormal hematopoiesis.

To examine the proteolytic efficiency of this AuNP-based microreactor for real case samples of biological complexity,

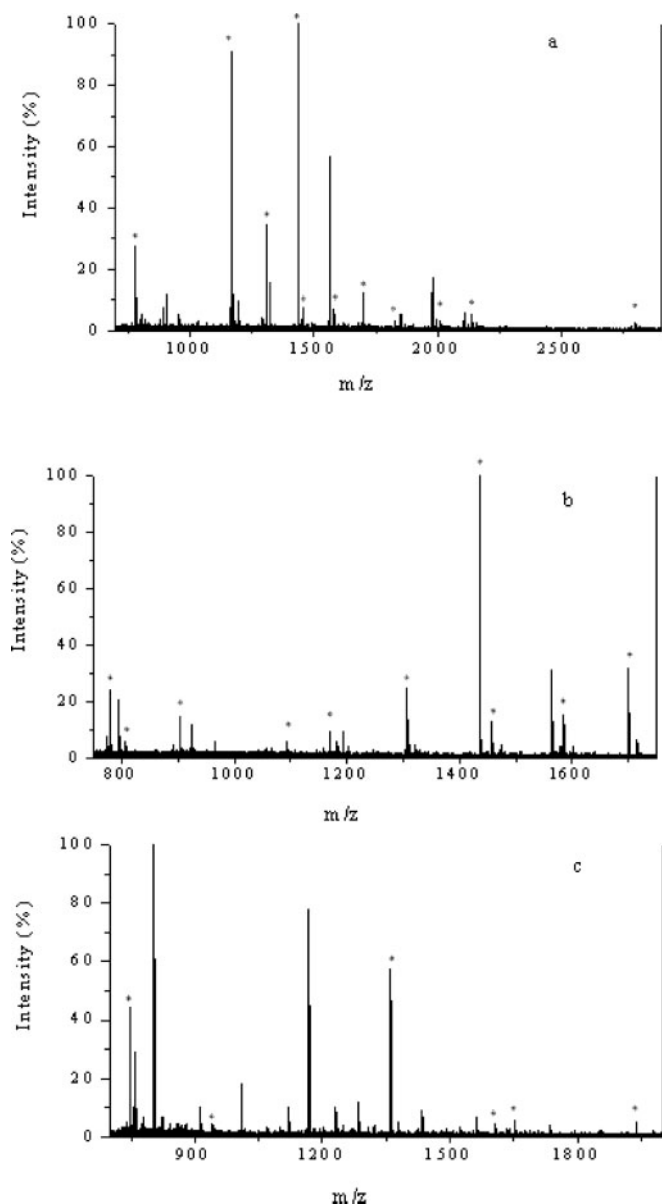


FIG. 5. a, MALDI-TOF mass spectrum of digests of 2 ng/ $\mu$ l Cyt-c. b, MALDI-TOF mass spectrum of digests of 0.5 ng/ $\mu$ l Cyt-c. c, MALDI-TOF mass spectrum of digests of 2 ng/ $\mu$ l myoglobin using PDDA/gold nanoparticle multilayer-modified microchip reactor with a flow rate of 2.0  $\mu$ l/min. The eluent-to-matrix ratio is 1:1. The peaks marked with asterisks represent the matched peptides.

we compared the proteolytic profile of on-chip *versus* in-solution digestion of proteins extracted from mouse macrophages by water. At a flow rate of 100  $\mu$ l/h, the cell extracts (2  $\mu$ g/ $\mu$ l) were digested in the immobilized enzyme microchip reactor within an incubation time of only 1 min followed by SCX-RPLC-ESI-MS-MS with a 145-min gradient elution for further isolation and identification. For comparison, the same protein extracts were incubated in trypsin solution for 6 h (the ratio of enzyme to protein was 1:30), and the digests were separated under the same condition as mentioned above. In

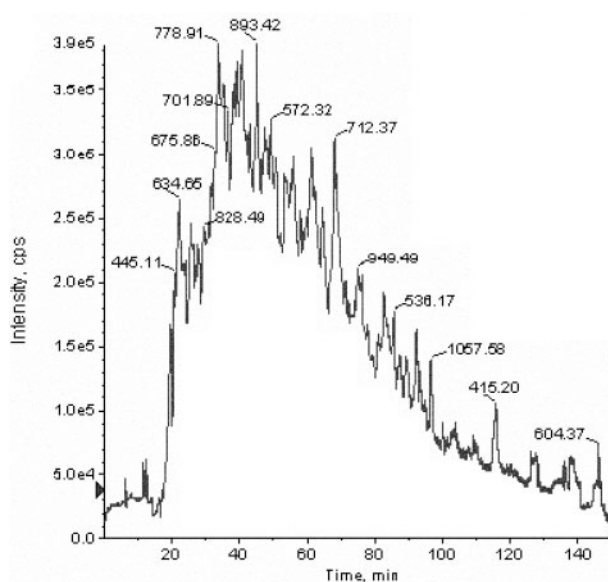


FIG. 6. Base peak chromatogram for separation of mouse macrophage protein digests by the microchip reactor for an incubation of 1 min. The digests of about 10  $\mu$ g of protein were analyzed by SCX-RPLC-MS/MS. The sample was 10  $\mu$ l of protein mixture extracted from mouse macrophages by urea in 50 mM Tris-HCl buffer (pH 8.1). See "Experimental Procedures" for detailed separation conditions. cps, counts per second.

Supplemental Fig.SI-3, the base peak chromatogram shows far more peptide signals resulting from on-chip digestion (Supplemental Fig. SI-3a) than in-solution digestion (Supplemental Fig.SI-3b). Using MS/MS peptide sequencing with stringent criteria for protein identification, a total of 149 and 162 proteins could be positively identified by on-chip and in-solution protocols, respectively. These results clearly show that this on-line microchip digestion is comparable to conventional in-solution digestion, but the incubation time is largely shortened to 1 min, and thus the proteolysis efficiency is significantly improved.

In addition, more protein fractions could be isolated from mouse macrophages denatured by urea, which is also likely to deactivate enzyme. To test whether urea has a side effect on the enzyme immobilized on the AuNPs within the microchannel, proteins extracted by urea were digested using our protocol, and then the resulting digests were subjected to the SCX-RPLC-ESI-MS/MS separation system. Fig. 6 is the base peak chromatogram of the on-chip digestion protocol. According to the searching criteria set above, the scores of 580 proteins were over the threshold of MASCOT-generated scores as individual protein scores  $>28$  indicate the identity or extensive homology ( $p < 0.05$ ). To further enhance the reliability of the identified proteins, we utilized the reversed IPI mouse version 3.07 database to evaluate the searching results (21, 22). As shown in Supplemental Fig. SI-4, after reverse database evaluation, the confidences  $p < 0.05$  and  $p < 0.01$  were assigned to those peptides when their corresponding scores were over 25 and 35, respectively. Therefore, MAS-

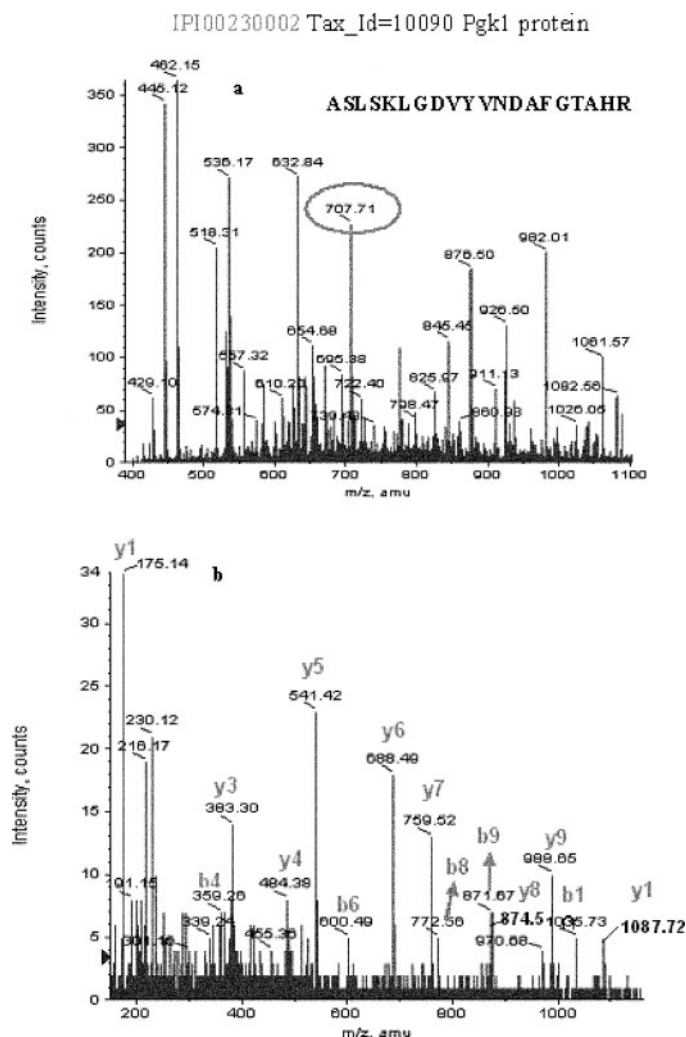


FIG. 7. *a*, PMF spectrum of Pgk 1 protein. *b*, the MS/MS spectrum of the  $m/z$  707.1.

COT-generated scores  $>28$  were considered as the filter, and only top rank peptide hits for given precursors were used. Proteins that matched two or more such effective peptides were reserved as validated identifications. It is worth noting that 99% (peptide score  $>35$ ) confidence as validated identification was required when proteins that matched one single peptide had a MASCOT score over 28. As a result, 497 proteins were identified. For example, Fig. 7a is the PMF spectrum of Pgk 1 protein, and Fig. 7b is the corresponding MS/MS spectrum of the  $m/z$  707.1; both show good signal-to-noise ratio. Supplemental Fig. SI-5 displays the molecular weight and isoelectric point distribution of the identified proteins. These results show that the on-chip digestion is feasible; the digestion time is reduced and operation procedures are simplified, both of which can favor rapid protein identification.

In addition to the larger surface-to-volume ratio and shorter diffusion time, the microchannel device exhibits a very small volume (about 50 nL/cm) and uniform flow. The enhanced

proteolytic efficiency might be due to the rapid mass transport properties in microchannels. In this study, we selected the macrophage cell line AMJ2-C8 to demonstrate the feasibility of the PDDA/AuNP multilayer-assembled microfluidic chips in the digestion of real samples. The analysis of protein complex mixtures isolated from a variety of biological systems will be investigated further. We expect that this microchip digestion system would be used for real time, large scale, and high throughput on-line protein analysis. Additionally although in the current work only the trypsin-immobilized PET on-chip reactor system was exemplified, the versatile applications of this AuNP modification protocol in other microchip devices are promising.

**Conclusion**—A sensitive on-chip digestion protocol for protein identification was proposed. The PDDA/AuNP multilayer assembly constructed on the surface of a PET microfluidic chip offers a biocompatible interface with large surface area, which is desirable for the controlled adsorption of trypsin. Due to a high concentration of trypsin confined in the microscopic microchannel, low levels of standard protein samples could be rapidly digested on the microchip reactor within a few seconds. Furthermore the performance of the on-line microchip bioreactor was illustrated by the digestion of real protein mixtures isolated from mouse macrophages. 497 proteins were identified by means of the combination of two-dimensional HPLC and ESI-MS/MS. One of the most outstanding advantages is that the enzyme-coated microchip could couple with LC-MS to implement on-line protein identification. Therefore, this proposed method is feasible in the characterization of various real sample extracts. Further investigation of the enzymatic reactor coupled with LC or off-gel techniques for on-line protein separation, digestion, and identification is underway in our laboratory.

**Acknowledgments**—We thank Dr. B. Su for helpful discussion, V. Devaud for technical help, and D. Yun for data searching.

\* This work was supported by National Natural Science Foundation of China Grants 20575013 and 20525519, 973 Program 2007CB714506, and the China-Swiss Science and Technology Cooperation Program. The costs of publication of this article were defrayed in part by the payment of page charges. This article must therefore be hereby marked "advertisement" in accordance with 18 U.S.C. Section 1734 solely to indicate this fact.

§ The on-line version of this article (available at <http://www.mcponline.org>) contains supplemental material.

§ Both authors made equal contributions to this work.

\*\* To whom correspondence should be addressed. Tel.: 86-21-65642405; Fax: 86-21-65641740; E-mail: bhliu@fudan.edu.cn.

#### REFERENCES

- Persidis, A. (1997) Proteomics—an ambitious drug development platform attempts to link gene sequence to expressed phenotype under various physiological states. *Nat. Biotechnol.* **16**, 393–394
- Copper, J. W., Chen, J. Z., Li, Y., and Lee, C. S. (2003) Membrane-based nanoscale proteolytic reactor enabling protein digestion, peptide separation, and protein identification using mass spectrometry. *Anal. Chem.* **75**, 1067–1074
- Sakai-Kato, K., Kato, M., and Toyooka, T. (2002) On-line trypsin-encapsu-



- lated enzyme reactor by the sol-gel method integrated into capillary electrophoresis. *Anal. Chem.* **74**, 2943–2949
4. Slysz, G. W., Lewis, D. F., and Schriemer, D. C. (2006) Detection and identification of sub-nanogram levels of protein in a nanoLC-trypsin-MS system. *J. Proteome Res.* **5**, 1959–1966
  5. Craft, D., Doucette, A., and Li, L. (2002) Microcolumn capture and digestion of proteins combined with mass spectrometry for protein identification. *J. Proteome Res.* **1**, 537–547
  6. Qin, J. H., Ye, N. N., Liu, X., and Lin, B. C. (2005) Microfluidic devices for the analysis of apoptosis. *Electrophoresis* **26**, 3780–3788
  7. Lion, N., Rohner, T. C. Dayon, L., Arnaud, I. L., Damoc, E., Youhnovski, N., Wu, Z., Roussel, C., Josserand, J., Jensen, H., Rossier, J. S., Przybylski, M., and Girault, H. H. (2003) Microfluidic systems in proteomics. *Electrophoresis* **24**, 3533–3562
  8. Calleri, E., Temporini, C., Perani, E., Palma, A. D., Lubda, C., Mellerio, G., Sata, A., Galliano, M., Caccialanza, G., and Massolini, G. (2005) Trypsin-based monolithic bioreactor coupled on-line with LC/MS/MS system for protein digestion and variant identification in standard solutions and serum samples. *J. Proteome Res.* **4**, 481–490
  9. Anderson, N. L., Haines, L. R., and Pearson, T. W. (2004) An effective and rapid method for functional characterization of immunoabsorbents using POROS beads and flow cytometry. *J. Proteome Res.* **3**, 228–234
  10. Peterson, D. S., Rohr, T., Svec, F., and Fréchet, J. M. J. (2002) High-throughput peptide mass mapping using a microdevice containing trypsin immobilized on a porous polymer monolith coupled to MALDI TOF and ESI TOF mass spectrometers. *J. Proteome Res.* **1**, 563–568
  11. Peterson, D. S., Rohr, T., Svec, F., and Fréchet, J. M. J. (2002) Enzymatic microreactor-on-a-chip: Protein mapping using trypsin immobilized on porous polymer monoliths molded in channels of microfluidic devices. *Anal. Chem.* **74**, 4081–4088
  12. Qu, H. Y., Wang, H. T., Huang, Y., Zhong, W., Lu, H. J., Kong, J. L., Yang, P. Y., and Liu, B. H. (2004) Stable microstructured network for protein patterning on a plastic microfluidic channel: strategy and characterization of on-chip enzyme microreactors. *Anal. Chem.* **76**, 6426–6433
  13. Wu, H. L., Tian, Y. P., Liu, B. H., Lu, H. J., Wang, X. Y., Zhai, J. J., Jin, H., Yang, P. Y., Xu, Y. M., and Wang, H. H. (2004) Titania and alumina sol-gel-derived microfluidics enzymatic-reactors for peptide mapping: design, characterization, and performance. *J. Proteome Res.* **3**, 1201–1209
  14. Liu, Y., Lu, H. J., Zhong, W., Song, P. Y., Kong, J. L., Yang, P. Y., Girault, H. H., and Liu, B. H. (2006) Multilayer-assembled microchip for enzyme immobilization as reactor toward low-level protein identification. *Anal. Chem.* **78**, 801–808
  15. Huang, Y., Shan, W., Liu, B. H., Liu, Y., Zhang, Y. H., Zhao, Y., Lu, H. J., Tang, Y., and Yang, P. Y. (2006) Zeolite nanoparticle modified microchip reactor for efficient protein digestion. *Lab Chip* **6**, 534–539
  16. Merkoci, A., Marta, A., Tarraso'n, G., Eritja, R., and Alegret, S. (2005) Toward an ICPMS-linked DNA assay based on gold nanoparticles immunocoupled through peptide sequences. *Anal. Chem.* **77**, 6500–6503
  17. Roberts, M. A., Rossier, J. S., Rercier, P., and Girault, H. H. (1997) UV laser machined polymer substrates for the development of microdiagnostic systems. *Anal. Chem.* **69**, 2035–2042
  18. Grabar, K. C., Freeman, R. G., Hommer, M. B., and Natan, M. J. (1995) Preparation and characterization of Au colloid monolayers. *Anal. Chem.* **67**, 735–743
  19. Chen, W., and McCarthy, T. J. (1997) Layer-by-layer deposition: a tool for polymer surface modification. *Macromolecules*, **30**, 78–86
  20. Gu, S., Liu, Z. H., Pan, S. Q., Jiang, Z. Y., Lu, H. M., Amit, O., Bradbury, E. M., Hu, C. A. A., and Chen, X. (2004) Global investigation of p53-induced apoptosis through quantitative proteomic profiling using comparative amino acid-coded tagging. *Mol. Cell. Proteomics* **3**, 998–1008
  21. Cargile, B. J., Bundy, J. L., and Stephenson, J. L. (2004) Potential for false positive identifications from large databases through tandem mass spectrometry. *J. Proteome Res.* **3**, 1082–1085
  22. Moore, R. E., Young, M. K., and Lee, T. D. (2002) Qscore: an algorithm for evaluating SEQUEST database search results. *J. Am. Soc. Mass Spectrom.* **13**, 378–386
  23. Feng, S., Ye, M. L., Jiang, X. G., Jin, W. H., and Zou, H. F. (2006) Coupling the immobilized trypsin microreactor of monolithic capillary with  $\mu$ RPLC-MS/MS for shotgun proteome analysis. *J. Proteome Res.* **5**, 422–428
  24. Calleri, E., Temporini, C., Perani, E., Stella, C., Rudaz, S., Lubda, D., Mellerio, G., Veuthey, J. L., Caccialanza, G., and Massolini, G. (2004) Development of a bioreactor based on trypsin immobilized on monolithic support for the on-line digestion and identification of proteins. *J. Chromatogr. A* **1045**, 99–109
  25. Lionello, A., Josserand, J., Jensen, H., and Girault, H. H. (2005) Protein adsorption in static microsystems: effect of the surface to volume ratio. *Lab Chip* **5**, 254–260
  26. Lionello, A., Josserand, J., Jensen, H., and Girault, H. H. (2005) Dynamic protein adsorption in microchannels by “stop-flow” and continuous flow. *Lab Chip* **5**, 1096–1103
  27. Van der Plancken, I., Van Remoortere, M., Indrawati, I., Van Loey, A., and Hendrickx, M. E. (2003) Heat-induced changes in the susceptibility of egg white proteins to enzymatic hydrolysis: a kinetic study. *J. Agric. Food Chem.* **51**, 3819–3823
  28. MacCoss, M. J., McDonald, W. H., Saraf, A., Sadygov, R., Clark, J. M., Tasto, J. J., Gould, K. L., Wolters, D., Washburn, M., Weiss, A., Cork, J. I., and Yates, J. R. (2002) Shotgun identification of protein modifications from protein complexes and lens tissue. *Proc. Natl. Acad. Sci. U. S. A.* **99**, 7900–7905
  29. Wilm, M., and Mann, M. (1996) Analytical properties of the nano-electrospray ion source. *Anal. Chem.* **68**, 1–8
  30. Park, Z. Y., and Russell, D. H. (2000) Thermal denaturation: a useful technique in peptide mass mapping. *Anal. Chem.* **72**, 2667–2670
  31. Chen, C. W., Boylan, M. T., Evans, C. A., Whetton, A. D., and Wright, E. G. (2005) Application of two-dimensional difference gel electrophoresis to studying bone marrow macrophages and their in vivo responses to ionizing radiation. *J. Proteome Res.* **4**, 1371–1380